



Poisson skeleton Revisited: A new mathematical perspective

Gilles Aubert, Jean-François Aujol

► To cite this version:

Gilles Aubert, Jean-François Aujol. Poisson skeleton Revisited: A new mathematical perspective. Journal of Mathematical Imaging and Vision, 2014, 48 (1), pp.149-159. hal-00714250

HAL Id: hal-00714250

<https://hal.science/hal-00714250>

Submitted on 4 Jul 2012

HAL is a multi-disciplinary open access archive for the deposit and dissemination of scientific research documents, whether they are published or not. The documents may come from teaching and research institutions in France or abroad, or from public or private research centers.

L'archive ouverte pluridisciplinaire **HAL**, est destinée au dépôt et à la diffusion de documents scientifiques de niveau recherche, publiés ou non, émanant des établissements d'enseignement et de recherche français ou étrangers, des laboratoires publics ou privés.

Poisson skeleton

Gilles Aubert ¹ & Jean-François Aujol ²

¹ Laboratoire J.A.Dieudonné, UMR CNRS 6621
Université de Nice Sophia-Antipolis
email: gaubert@math.unice.fr

² IMB, UMR CNRS 5251, Université Bordeaux 1,
email: Jean-Francois.Aujol@math.u-bordeaux1.fr

July 3, 2012

Abstract

This paper is concerned with the computation of the skeleton of a shape Ω included in \mathbb{R}^2 . We show some connections between the Euclidean distance function d to $\partial\Omega$ and the solution u of the Poisson problem $\Delta u(x) = -1$ if x is in Ω and $u(x) = 0$ if x is on $\partial\Omega$. This enables us to propose a new and fast algorithm to compute an approximation of the skeleton of $\partial\Omega$. We illustrate the approach with some numerical experiments.

Key-words: Skeleton, Poisson equation, distance function, PDEs, ODEs.

1 Introduction

One of the goal of shape analysis is to describe objects with a minimal amount of information. Skeletonization answers this question. The skeleton or medial axis of a shape gives a thin topologically equivalent representation of the original shape. The importance of skeleton was discussed by Blum [3, 4] with motivation from visual perception. Nowadays skeletonization is frequently used in computer vision and pattern recognition. There exist several ways (more or less equivalent) to define the skeleton of a shape in the real plane (see for example [6] for a quick survey and references on the subject). The first one goes back to [3, 4] whose author has introduced the concept of prairie fire in which the shape is imagined to be filled with dry grass and the fire is started at the shape boundary. The boundary propagates with constant normal velocity and the skeleton is traced out by the singular points where the front intersects itself. Another approach is to consider

the skeleton as the geometric location of centers of maximal discs contained in the shape [3, 5]. This definition is interesting since, in principle, if the radii of these discs are recorded at the corresponding points on the skeleton, the shape can be recovered as the envelope of all the discs centered on the skeleton with radii recorded. However, in practice, this approach is difficult to implement numerically. A third approach is to consider the skeleton as the set where the gradient of the distance function to the shape is discontinuous. If Ω denotes the shape, the signed distance to Ω is defined, for $x \in \mathbb{R}^2$, by $d(x) = d(x, \partial\Omega) = \inf_{y \in \partial\Omega} \|x - y\|$ where $\|x\|$ is the Euclidean norm of x . It is well known that the gradient of the distance function satisfies the eikonal equation $\|\nabla d(x)\| = 1$ except at points x where there exist at least two distinct points y and $z \in \partial\Omega$ such that $d(x) = \|x - y\| = \|x - z\|$. The set of such points x form the skeleton and at that points ∇d is discontinuous. We choose this last definition of the skeleton in the rest of the paper and we refer to it as the real skeleton.

The challenge is how to compute the skeleton or an approximation of it. There exist in the literature many different approaches on this issue. Let us only quote some of them: the morphological approach [17, 22, 18, 20], the wavelet approach [27] and those which are embedded in a partial differential equation (PDE) or variational framework [24, 7, 26, 14]. In these four last papers the authors highlight the connection between monotonically evolving fronts and the eikonal equation and they propose various algorithms for tracking shocks. It is well-known that hyperbolic PDEs (as the eikonal equation) are not easy to solve numerically and very fine algorithms must be used. A different but related point of view is given in [25] where the authors construct a function v whose level curves mimic the curve evolution with a speed consisting of a constant component and a component proportional to curvature. The function v is defined as the minimizer of a Modica-Mortola type functional [19] which approximates the perimeter of the boundary of the shape. The smoothed skeleton is then defined as the locus of points where the gradient of v is minimum along the level curves. Our contribution is in the same spirit as the works mentioned above but we think that our model is significantly simpler since it is based on the resolution of the well-known second order PDE: the Poisson equation $\Delta u(x) = -1$ with Dirichlet boundary conditions. More precisely if Ω denotes the shape we want to analyze, our algorithm is as follows:

1. We solve the Poisson equation $\Delta u(x) = -1$ in Ω , $u = 0$ on $\partial\Omega$.
2. We determine the set

$$\mathcal{A} = \{x \in \partial\Omega, \text{ the curvature of } \partial\Omega \text{ in } x \text{ has local maximum}\} \quad (1)$$

3. For each $x \in \mathcal{A}$, we solve the dynamical system

$$\begin{cases} \xi'(s) = \nabla u(\xi(s)) \\ \xi(0) = x \end{cases} \quad (2)$$

We denote by \mathcal{S}_1 the set of trajectories of these flows.

4. Let us define the sets W , E , and F :

$$W = \{x \in \Omega, \nabla u(x) = 0\} = E \bigcup F \quad (3)$$

$$E = \{x \in \Omega, \nabla u(x) = 0, \lambda_1 \leq \lambda_2 < 0\} \quad (4)$$

$$F = \{x \in \Omega, \nabla u(x) = 0, \lambda_1 < 0 \leq \lambda_2\} \quad (5)$$

where λ_1 and λ_2 are the eigenvalues of $\nabla^2 u$ (λ_i is real since $\nabla^2 u$ is symmetric real). W is the set of critical points of u in Ω . E is the set of extremal points of u in Ω (which in fact are maximal points since $\Delta u = -1$) and F is the set of saddle points of u in Ω . We set \mathcal{S}_2 the trajectories from F to E (see Section 5 for more details).

5. The skeleton of Ω is defined by

$$\mathcal{S} = \mathcal{S}_1 \bigcup \mathcal{S}_2 \bigcup W \quad (6)$$

Let us explain briefly why this algorithm furnishes an approximation of the real skeleton. The justification comes from four facts which will be proved in the next sections.

1. Actually the solution of the Poisson equation $\Delta u(x) = -1$ in Ω , $u = 0$ on $\partial\Omega$, can be viewed as a regularization of the distance function d .
2. As shown in [15, 14] the real skeleton tends to terminate at the boundary at points of maximal curvature.
3. If d is the distance function and if locally we parameterize the real skeleton by a curve $\xi(s)$ then necessarily $\xi(s)$ satisfies the dynamical system

$$\xi'(s) = \nabla d(\xi(s)) \quad (7)$$

where here the gradient ∇d of d has to be understood in a generalized sense. Actually d is a function of bounded variations and a meaning can be given to system (7) (see [2]).

4. The trajectories defined in (2) converge asymptotically as $s \rightarrow \pm\infty$ to points in the critical set W which is finite.

Let us point out that Poisson equation has already been used in shape representation. In [10] the authors utilize the gradient and the curvature of the level sets of the solution of Poisson equation for segmenting silhouette, identifying corners and deriving some structures of the skeleton of a shape. In that paper no real mathematical justification is given. Let us also note that Poisson equation is related to the Brownian motion of a set of particles placed inside the shape. Indeed the solution u of Poisson equation measures the mean time required for a particle to hit the boundary [12].

The paper is organized as follows. In Section 2 we first recall classical properties of Poisson equation. Then in Section 3 we give some reasons why u the solution of Poisson equation can be viewed as a regularization of the distance function. In Section 4 we study the dynamical system (2) and in particular its asymptotic behaviour as $s \rightarrow \pm\infty$. Then in Section 5 we write the detailed algorithm. Finally we illustrate the capability of our algorithm in Section 6 by showing several computational examples.

2 Some results about Poisson equation

2.1 Classical results

In this section we recall some well-known properties of the solution u of Poisson equation:

$$\Delta u(x) = -1 \text{ if } x \text{ is in } \Omega, u=0 \text{ on } \partial\Omega. \quad (8)$$

Proposition 1 • Existence and uniqueness: *If $\partial\Omega$ is Lipschitz then (8) admits a unique solution u in the Sobolev space $W_0^{1,p}(\Omega)$, $\forall p \in [2, \infty[$.*

- Regularity: *If $\partial\Omega$ is of class C^2 , then u is in $C^2(\bar{\Omega})$.*
- Maximum principle: *There exists $C > 0$ such that $0 \leq u \leq C$ on $\bar{\Omega}$. Moreover, we have $0 < u$ on Ω .*

Proof: See [8, 9].

■

As a consequence of Proposition 1, we can then extend u as a C^2 function on \mathbb{R}^2 . This is what we do until the end of the paper (so we suppose that $\partial\Omega$ is of class C^2).

2.2 More refined properties

We set $\lambda_1 \leq \lambda_2$ the eigenvalues of $\nabla^2 u$ (λ_i is real since $\nabla^2 u$ is symmetric real). In Ω , we have $\Delta u = -1 = \lambda_1 + \lambda_2$. Hence $\lambda_1 < 0$.

Let us consider the set W , E , and F defined by (3), (4) and (5). W is the set of critical points of u in Ω . E is the set of extremal points of u in Ω (which in fact are maximal points since $\Delta u = -1$) and F is the set of saddle points of u in Ω . We give below a nontrivial result due to Alessandrini et al [1] concerning the number of critical points of u . This result is fundamental for our algorithm.

Theorem 1 *Let us assume that Ω is a simply connected open set in \mathbb{R}^2 . W is a non empty set, and W contains at most a finite number of points (which are isolated). Moreover, we have $\#E - \#F = 1$.*

Remarks:

1. If Ω is convex, then W is reduced to a single point which is the maximizer of u on Ω [16].

For example [13], if Ω is symmetric and convex in two orthogonal directions, then all the level sets of u are symmetric and convex in those directions, and they are star-shaped. Under those assumptions, the gradient of u vanishes only in a single point, the center of symmetry.

2. If Ω is not simply connected then W can be a curve. For example if Ω is the annulus $\Omega = \{(x, y); 1 \leq x^2 + y^2 \leq 4\}$. It is easy to see that $u(x, y) = \frac{3}{8 \log 2} \log(x^2 + y^2) - \frac{1}{4}(x^2 + y^2 + \frac{1}{4})$ is the solution of (8) and

$$u_x = \frac{3}{4 \log 2} \frac{x}{x^2 + y^2} - \frac{1}{2}x \quad (9)$$

$$u_y = \frac{3}{4 \log 2} \frac{y}{x^2 + y^2} - \frac{1}{2}y \quad (10)$$

Moreover, we have: $\nabla u(x, y) = (0, 0)$ if and only if $x^2 + y^2 = \frac{3}{2 \log 2} \approx 2.16$ (notice that $(0, 0)$ does not belong to Ω). Hence the set of critical points is a circle of radius $\sqrt{2.16} \approx 1.47$. It is close to 1.5, but not equal to it.

Corollary 1 *If x is in W and Ω simply connected, then x is a non degenerated points, i.e. $\lambda_1 \neq 0$ and $\lambda_2 \neq 0$.*

Proof: If one of the eigenvalue is zero, then there exist non isolated critical points (see [11] page 326), which contradicts Theorem 1. ■

Remark: As a consequence, F (defined by (5)) is in fact :

$$F = \{x \in \Omega, \nabla u(x) = 0, \lambda_1 < 0 < \lambda_2\} \quad (11)$$

Proposition 2 *There exists $\alpha > 0$ such that $\nabla u \cdot N \geq \alpha$ on $\partial\Omega$, with N the inner normal to $\partial\Omega$.*

Proof: This is a consequence of the Hopf lemma [8], and of the fact that $\partial\Omega$ is C^2 and Ω bounded. ■

Corollary 2 *Let β in $(0, \alpha)$ (with α given by Proposition 2). Then there exists $r > 0$ such that $\nabla u \cdot N_r \geq \beta$ on $\partial\Omega_r$, with N_r the inner normal to $\partial\Omega_r$, and*

$$\Omega_r = \{x \in \Omega, d(x, \Omega) \geq r\} \quad (12)$$

Proof: This is a consequence of the fact that u is in $C^2(\mathbb{R}^2)$ and of Proposition 2. ■

3 Relating the Poisson equation with the distance function

In this section we give some heuristic reason showing the connection between the solution of the Poisson equation and the distance function. Further connection will be explained in Section 5. In all this section we denote by

$u(x)$ the unique solution of Poisson equation:

$$\Delta u(x) = -1 \text{ if } x \text{ is in } \Omega, u(x)=0 \text{ on } \partial\Omega. \quad (13)$$

Now for $\epsilon > 0$, let us consider the following PDE:

$$\begin{cases} \epsilon \frac{\partial z}{\partial t}(x, t) = \Delta z(x, t) + 1 \text{ in } \Omega \times (0, \infty) \\ z(x, t) = 0 \text{ on } \partial\Omega \times (0, \infty) \\ z(x, 0) = d(x) \end{cases} \quad (14)$$

From [8], equation (14) admits a unique regular solution $z_\epsilon(x, t)$.

Thanks to (13), equation (14) can be written into

$$\begin{cases} \epsilon \frac{\partial z}{\partial t}(x, t) = \Delta z(x, t) - \Delta u(x) \text{ in } \Omega \times (0, \infty) \\ z(x, t) = 0 \text{ on } \partial\Omega \times (0, \infty) \\ z(x, 0) = d(x) \end{cases} \quad (15)$$

Setting $w_\epsilon(x, t) = z_\epsilon(x, t) - u(x)$ then $w_\epsilon(x, t)$ is a solution of the following heat equation:

$$\begin{cases} \epsilon \frac{\partial w_\epsilon}{\partial t}(x, t) = \Delta w_\epsilon(x, t) \text{ in } \Omega \times (0, \infty) \\ w_\epsilon(x, t) = 0 \text{ on } \partial\Omega \times (0, \infty) \\ w_\epsilon(x, 0) = d(x) - u(x) \end{cases} \quad (16)$$

From classical estimations [8] for the heat equation we get the following estimate:

$$\|w_\epsilon(\cdot, t)\|_{L^2(\Omega)} \leq \|d - u\|_{L^2(\Omega)} e^{-(\mu_1 t/\epsilon)} \quad (17)$$

where μ_1 is the first eigenvalue of the Laplacian. From (17) we deduce when $\epsilon \rightarrow 0^+$ that for all $t > 0$ then $z_\epsilon(\cdot, t) \rightarrow u(\cdot)$. Therefore this convergence shows that $z_\epsilon(x, t)$ is close to $u(x)$ for ϵ small and for all $t > 0$. But for small $t > 0$, $z_\epsilon(x, t)$ can be viewed as a smoothed version of the distance function $d(x)$. Thus these heuristic arguments show some connection between the solution of the Poisson equation and the distance function. More arguments will be given later in section 5.

4 Study of the dynamical system

In this section we first study the gradient flow (2) associated to u and then we justify why its trajectories can be used as an approximation of the skeleton. From now on, we assume that the shape Ω is a simply connected open set (thus the points in W are isolated thanks to Theorem 1).

4.1 Definitions and basic results

We consider the following problem. Let x_0 in $\bar{\Omega}$, and:

$$\begin{cases} \xi'(s) = \nabla u(\xi(s)) \\ \xi(0) = x_0 \end{cases} \quad (18)$$

where u is the unique solution of (8).

Remark: Notice that if $x_0 \in W$, then $\xi(s) = x_0$ for all s in \mathbb{R} .

Proposition 3 *There exists a unique C^1 function ξ solution of (18). This solution is defined on \mathbb{R} .*

Proof: The uniqueness of ξ is given by Cauchy-Lipschitz theorem for ODE. The existence on \mathbb{R} is standard, since ∇u remains bounded on \mathbb{R}^2 . ■

From Theorem 1, we know that the set of critical points of ∇u are isolated points. Moreover, we saw that $W = \{x \in \Omega, \nabla u(x) = 0\} = E \cup F$, with E the set of maximal points of u in Ω , and F the set of saddle points of u in Ω .

Let us now state some basic results about the qualitative property of (18) in a neighbourhood of a point in E .

Proposition 4 *If x is in E , then x is an attractive point. There exists $r > 0$ such that if x_0 belongs to $B(x, r)$ (the ball of radius r centered in x), then $\xi(s) \rightarrow x$ as $s \rightarrow +\infty$.*

Proof: See Theorem 8.4 page 366 of [11].

■

Proposition 5 *If x is in F , then x is a saddle point, and we have the following properties :*

1. *There exists exactly two trajectories ξ_i , $i = 1, 2$, such that $\xi_i(s) \rightarrow x$ as $s \rightarrow +\infty$.*
2. *There exists exactly two trajectories ξ_i , $i = 1, 2$, such that $\xi_i(s) \rightarrow x$ as $s \rightarrow -\infty$.*

Proof: See Theorem 8.5 page 371 of [11].

■

Corollary 3 *Let us consider ξ the unique solution of (18).*

1. *Let us assume that there exists an increasing sequence s_n such that $s_n \rightarrow +\infty$, and $\xi(s_n)$ converges to some element w of W . Then $\xi(s) \rightarrow w$ as $s \rightarrow +\infty$.*
2. *Let us assume that there exists a decreasing sequence s_n such that $s_n \rightarrow -\infty$, and $\xi(s_n)$ converges to some element w of W . Then $\xi(s) \rightarrow w$ as $s \rightarrow -\infty$.*

Proof: We first remark that the points of W are isolated thanks to Theorem 1. The rest of the proof is a straightforward consequence of Propositions 4 and 5.

■

4.2 Qualitative results

The next theorem states the following fact: given a point x_0 in $n \bar{\Omega} \setminus W$, there exists a trajectory of the flow (18) such that when $s \rightarrow +\infty$, $\xi(s) \rightarrow y_\infty$ with y_∞ in W . Moreover, there exists s_0 in \mathbb{R}_+^* such that $\xi(s_0) \in \partial\Omega$ or $\xi(s) \rightarrow z_{-\infty} \in F$ as $s \rightarrow -\infty$.

Theorem 2 *Let x_0 in $\bar{\Omega} \setminus W$. The unique solution ξ of (18) satisfies the two following properties.*

1. $\xi(s)$ belongs to Ω for all $s > 0$. Moreover, there exists y_∞ in W (given by (3)) such that: $\xi(s) \rightarrow y_\infty$ as $s \rightarrow +\infty$.
2. One of the two following properties hold:
 - (a) There exists s_0 in \mathbb{R}_+^* such that $\xi(s_0)$ belongs to $\partial\Omega$, and $\xi(s) \in \mathbb{R}^2 \setminus \bar{\Omega}$ if $s < s_0$.
 - (b) $\xi(s)$ remains in Ω for all s in \mathbb{R} , and there exists $z_{-\infty}$ in F such that: $\xi(s) \rightarrow z_{-\infty}$ as $s \rightarrow -\infty$. Moreover, the set of elements x_0 , which satisfies this last property, is embedded into a finite number of curves.

Proof:

1. We begin by showing the first point of the proposition. The fact that $\xi(s)$ belongs to Ω for all $s > 0$ is a straightforward consequence of Proposition 2.

Let us consider y_0 in Ω such that $u(y_0) = \max_{x \in \bar{\Omega}} u(x)$ and let F be the function:

$$F(x) = \|u(x) - u(y_0)\|^2 \quad (19)$$

F is a Liapounov function for problem (18). Indeed, F has a minimum in y_0 , and if x is in Ω , $x \in \bar{\Omega} \setminus W$, then:

$$\langle \nabla F(x), \nabla u(x) \rangle = 2\|\nabla u(x)\|^2(u(x) - u(y_0)) < 0 \quad (20)$$

(using the fact that y_0 is a maximum of u). Assertion 1. is then a standard result on ODE (see [11] page 363 Theorem 8.2 and Remark page 364). For the convenience of the reader we detail the proof below.

We have:

$$\frac{d}{ds}(F(\xi(s))) = \langle \xi'(s), \nabla F(\xi(s)) \rangle = \langle \nabla u(\xi(s)), \nabla F(\xi(s)) \rangle \quad (21)$$

Hence:

$$\frac{d}{ds}(F(\xi(s))) = 2(u(\xi(s)) - u(y_0))\|\nabla u(\xi(s))\|^2 < 0 \quad (22)$$

for all $s \geq 0$ since $\xi(0) = x_0$ is not in W , so $s \mapsto F(\xi(s))$ is a strictly decreasing non negative function.

$\xi(s)$ belongs to $\bar{\Omega}$ for all $s \geq 0$, and Ω is bounded. Let us consider an increasing sequence s_n which goes to $+\infty$ as $n \rightarrow +\infty$. Let us denote $\xi(s_n)$ by ξ_n . (ξ_n) is a bounded sequence in $\bar{\Omega}$. Up to a subsequence, it is thus a convergent sequence.

$F(\xi_n)$ is a strictly decreasing non negative sequence. It is therefore a convergent sequence. In particular, we have $F(\xi_n) - F(\xi_{n+1}) \rightarrow 0$.

But we know that there exists t_n in (s_n, s_{n+1}) such that:

$$\frac{d}{ds}F(\xi(t_n)) = F(\xi_{n+1}) - F(\xi_n) \quad (23)$$

$\xi(t_n)$ is a bounded sequence. Hence, up to a subsequence, it is a converging sequence. Let us denote by y_∞ its limit. We have

$$\frac{d}{ds}F(y_\infty) = 0 \quad (24)$$

This implies with (22) that $\nabla u(y_\infty) = 0$ and so y_∞ belongs to W . We therefore have shown that any cluster point of ξ_n belongs to W . We conclude thanks to Corollary 3 that $\xi(s)$ converges to y_∞ .

Remark: If W is a singleton then $y_\infty = y_0$ (this is in particular the case when Ω is convex).

2. To show the second point, we first see that if there exists s_0 in \mathbb{R}_- such that $\xi(s_0)$ belongs to $\partial\Omega$, then $\xi(s) \in \mathbb{R}^2 \setminus \bar{\Omega}$ if $s < s_0$ (as a straightforward consequence of Proposition 2).

Let β in $(0, \alpha)$ as in Corollary 2. Then if there exists s_1 in \mathbb{R} such that $\xi(s_1)$ belongs to $\mathbb{R}^2 \setminus \Omega_r$, there exists s_0 in \mathbb{R}_- such that $\xi(s_0)$ belongs to $\partial\Omega$ (as a consequence of Corollary 2).

Now let us assume that $\xi(s)$ remains in Ω_r for all s in \mathbb{R} , and let us consider the function:

$$G(x) = \|u(x)\|^2 \quad (25)$$

G is a Liapounov function for problem (18) with reversed time. The rest of the proof is the same as before.

■

We have thus completely determined the behaviour of the trajectories of the flow (18). This is the basis of the algorithm we introduce in the next section.

5 Detailed algorithm

5.1 Our approach

In this section we describe our algorithm for constructing the Poisson skeleton of a shape Ω and we show more connection between that skeleton and the real skeleton constructed from the distance function.

We first define the set:

$$\mathcal{A} = \{x \in \partial\Omega, \text{ the curvature of } \partial\Omega \text{ in } x \text{ has local maximum.}\} \quad (26)$$

Then let u be the solution of Poisson equation (8) and the sets W , E and F defined respectively in (3), (4) and (5). For constructing the Poisson skeleton of Ω we consider the following flow starting from x in \mathcal{A} :

$$\begin{cases} \xi'(s) = \nabla u(\xi(s)) \\ \xi(0) = x \end{cases} \quad (27)$$

We denote by \mathcal{S}_1 the set of trajectories of these flows. Thanks to Theorem 2, we know that these trajectories converge to points in W . Of course, since the flow starts from x on $\partial\Omega$, we need to remove the beginning of these trajectories. Since x is in \mathcal{A} , it is easy to see that the length of the trajectory to be removed is equal to $1/\rho$, where ρ is the curvature of $\partial\Omega$ in x [14]. To compute flow (27), we use a dynamical programming approach. Given a point x on the flow, we compute the next point y on the flow, in the neighbourhood of x (8-neighbourhood of x in practice), as the point y for which $u(y)$ is minimum.

We set \mathcal{S}_2 the trajectories from F to E . If x is in F , then it is an unstable fixed point of the flow considered here. Thus, from a numerical point of view, one just need to select points in the neighbourhood of x (in 4 or 8 connexity), and to compute the trajectories from these points with the flow (27).

So the question remains on how to compute the location of the points in F . This could be done by computing the zeros of the function $x \mapsto \|\nabla u(x)\|^2$ in Ω . But we have found it to be more accurate to see the points in F as the points where the sign of the curvature changes as explained later.

Definition: The Poisson skeleton is defined as

$$\mathcal{S} = \mathcal{S}_1 \cup \mathcal{S}_2 \cup W \quad (28)$$

Let us explain why the Poisson skeleton can be regarded as an approximation of the real skeleton. The fact that the skeleton tends to terminate at points on the boundary of maximal curvature is well established in the computer vision community (see [15, 14]).

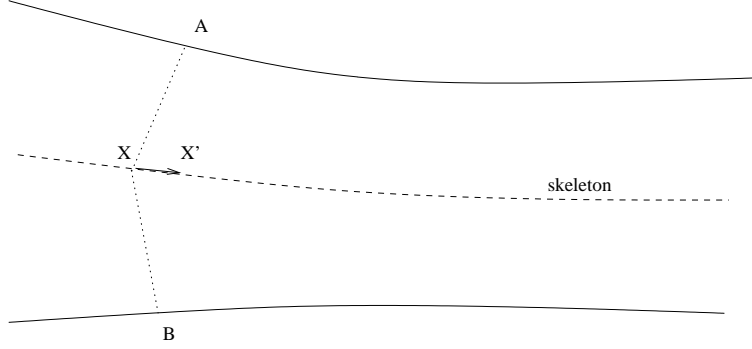


Figure 1: Local parameterization of the skeleton of an arbitrary shape. X is on the skeleton, and points A and B realize the distance of X to the boundary of the shape. The tangent vector X' is the bisector of the angle (XA, XB) , and the segment AB is orthogonal to X' .

But why using equation (27) ? Let us suppose that the real skeleton is given by a parameterized curve $X(t)$ and let be $X_0 = X(t_0)$ a point on the skeleton. By definition there exist two points A and B on the boundary $\partial\Omega$ such that $d(x_0, \partial\Omega) = \|X_0A\| = \|X_0B\|$. It can also be shown that the tangent $X'(t_0)$ is the bisector of the angle (X_0A, X_0B) and that the segment AB is orthogonal to $X'_0 = X'(t_0)$ (see Figure 1).

Let us now define $\nabla^+d(X_0)$ (respectively $\nabla^-d(X_0)$) as the gradient of the distance function in the direction AX_0 (respectively BX_0). It is easily seen that these vectors do exist and that the vector $(\nabla^+d(X_0) + \nabla^-d(X_0))$ is parallel to $X'(t_0)$. Let us denote $\nabla^\bullet d(X(t)) = \frac{1}{2}(\nabla^+d(X(t)) + \nabla^-d(X(t)))$. From the above considerations the vector $\nabla^\bullet d(X(t))$ is parallel to $X'(t)$ and this can be formally expressed as

$$\nabla^\bullet d(X(t)) = X'(t) \quad (29)$$

So we have just shown that if the skeleton is represented by a curve $X(t)$ then necessarily $X(t)$ satisfies (29) which is the flow (27) where u is replaced by d . We think that this observation fully justifies the construction of the Poisson skeleton.

Remarks:

1. From a mathematical point of view the writing of (29) can be justified. Actually the distance function belongs to the space $BV^2(\Omega) = \{f \in W^{1,1}(\Omega) ; \frac{\partial f}{\partial x_i} \in BV(\Omega) \text{ for } i = 1, \dots, n\}$ and $\nabla^\bullet d$ is called the *precise representation* of ∇d . In this setting it can be shown that (29) admits a solution in a generalized meaning (see [21, 2]).

2. Our construction of the Poisson skeleton shares some similarities with the one of Shah et al [23]. In that paper the authors define an approximation of the skeleton as the locus of points where the norm of the gradient of a smoothed distance function $v(x)$ is minimum along the level curves i.e. they solve $\frac{d\|\nabla v\|}{ds} = 0$ where s is the arc-length along the level curves of v . The smoothed distance v is constructed as the minimum of a Modica-Mortola functional. A direct computation shows that the equation $\frac{d\|\nabla v\|}{ds} = 0$ is equivalent to

$$\frac{v_{xy}(v_x^2 - v_y^2) - v_x v_y(v_{xx} - v_{yy})}{|\nabla v|^3} = 0 \quad (30)$$

But this expression is exactly the curvature of the trajectories defined in (27). Indeed, we have: $\xi'(s) = \nabla u(\xi(s))$, and thus $\xi''(s) = \nabla u(\xi(s))\xi'(s)$. We remind the reader that the curvature of a parametrized $s \mapsto \xi(s)$ is:

$$\kappa(s) = \frac{\xi_1' \xi_2'' - \xi_2' \xi_1''}{((\xi_1')^2 + (\xi_2')^2)^{3/2}} \quad (31)$$

So here $\xi_1' = u_x$, $\xi_2' = u_y$, $\xi_1'' = u_{xx}u_x + u_{yx}u_y$, $\xi_2'' = u_{xy}u_x + u_{yy}u_y$. Hence:

$$\kappa(s) = \frac{u_x(u_y u_{yy} + u_x u_{xy}) - u_y(u_x u_{xx} + u_y u_{yx})}{|\nabla u|^3} \quad (32)$$

i.e.:

$$\kappa(s) = \frac{u_{xy}(u_x^2 - u_y^2) - u_x u_y(u_{xx} - u_{yy})}{|\nabla u|^3} \quad (33)$$

which is precisely the expression (30) where v is replaced by u .

As will be seen in the next section on Figures 2 to 5, the sign of the curvature gives some indication on where the skeleton is (see [23] for further details). However, as pointed in [23], such an approach gives an approximation of both the skeleton and the anti skeleton: a pruning step is needed afterwards. Moreover, as can be seen Figures 2 to 5, our approach seems to lead to a better approximation of the skeleton in practice.

5.2 Basic examples for Ω

Here we detail basic examples of Ω where we can actually show that the skeleton computed with our algorithm is the true skeleton.

Circle In such a simple case, it is easy to see that our algorithm give the center of the circle as the unique element of the inner skeleton of the circle.

Ellipse Again it is easy to show that the center of the ellipse is the unique critical point of u and that $\frac{\partial u}{\partial y}(x, 0) = 0$. Moreover, Ω has only two points with maximal curvature: the summits corresponding to the largest radius of the ellipse.

Without any restriction, let us assume that the horizontal axis is the largest radius of the ellipse. Then, since $\frac{\partial u}{\partial y}(x, 0) = 0$, it implies that the trajectories starting from these two summits go straight to the center of the ellipse.

We conclude that in this particular case, our algorithm give the exact solution.

Square Since the diagonal are symmetry axis for Ω , and since the two diagonals are non parallel (in fact they are even orthogonal), we conclude with the same arguments as above that our algorithm provide the user with the exact solution.

Rectangle Unfortunately, even in such a simple example, it remains an open question to prove that the skeleton given by our algorithm is indeed an approximatin of the genuine skeleton. Nevertheless, as will be shown on Figure 4, our algorithm provide numerically a perfect result.

6 Numerical examples

In this section, we show some numerical examples to illustrate that indeed our algorithm gives a good approximation of the skeleton. As a comparison, we also give the sign of the curvature given by equation (33), which is the first step of the approach of [23].

Figures 2 to 5 present results on different simply connected shapes. Our algorithm gives a very good approximation in all cases. The reader should notice the difference between the skeleton provided by our method, and the information given by the sign of the curvature. One should also notice that the intersection of the boundary with the change of sign of the curvature gives a robust and accurate approximation of the location of the local maximum of the curvature along the boundary.

In Figure 2, we show the obtained result on a moon-like shape. In Figure 3, we show the obtained result on a star-like shape. These two examples are perfect matches for our algorithm.

In Figure 4, we show the obtained result on a rectangle. Notice that the method works although the rectangle boundary is not C^2 . In Figure 5, we show the obtained result on a complicated shape. One should notice that the approximate location of the stationary points of the flow are given by the location of the change of signs of the curvature.

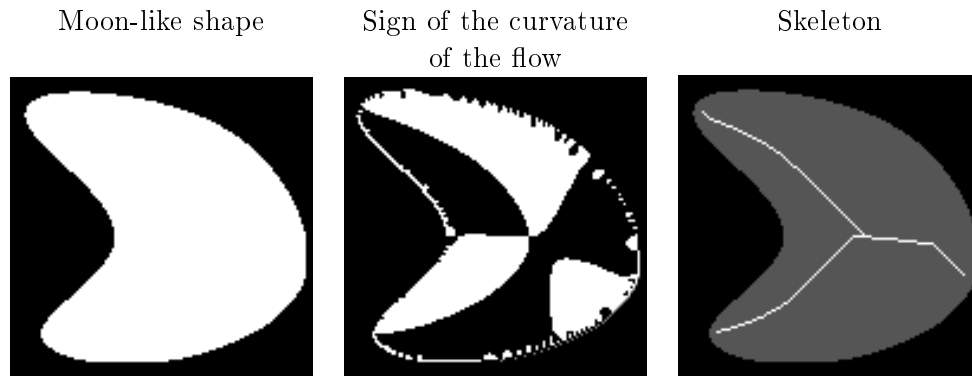


Figure 2: Skeleton computation of a moon-like shape. The change of sign of the curvature gives the location of the maximum of the curvature on the boundary of the shape.

We can notice that in all these examples the only one for which E is non void is the one given in Figure 5.

7 Conclusion

In this paper, we have proposed a novel algorithm to compute an approximation of the skeleton. Based on a mathematical analysis, we gave some insight on why such an approach is efficient. The Poisson equation has already been used to compute approximation of the skeleton in the computer vision community [23, 10]. We gave here new mathematical arguments to justify such an approach, and we have proposed a completely new algorithm that seems to perform well, as demonstrated in our numerical examples.

References

- [1] G. Alessandrini and R. Magnanini. The index of isolated critical points and solutions of elliptic equations in the plane. *Annali della Scuola Normale Superiore di Pisa*, 19(4):567–589, 1992.
- [2] L. Ambrosio. Transport equation and cauchy problem for non-smooth vector fields. In B. Dacorogna and P. Marcellini, editors, *Lecture Note in Mathematics*, volume 1927, pages 2–41, 2008.
- [3] H. Blum. A transformation for extracting new descriptors of shape. In Walthen Dunn, editor, *Models for the Perception of Speech and Visual Form*, volume 80, pages 362–380, 1967. MIT Press.

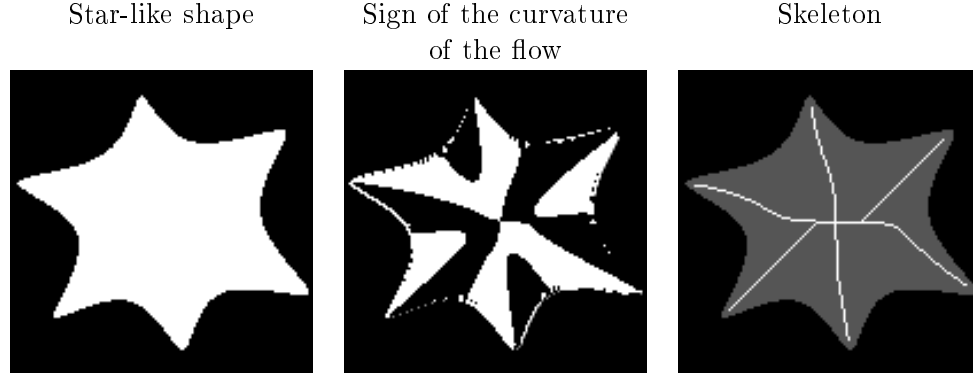


Figure 3: Skeleton computation of a star-like shape. This kind of shape is perfect for the framework developped in this paper.

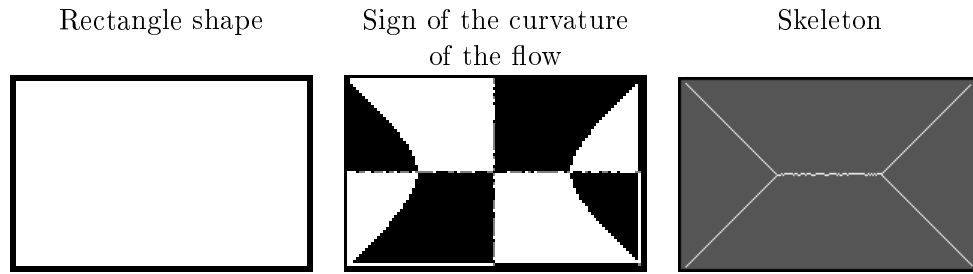


Figure 4: Skeleton computation of a rectangle shape. Although the boundary is not C^2 , our algorithm performs well.

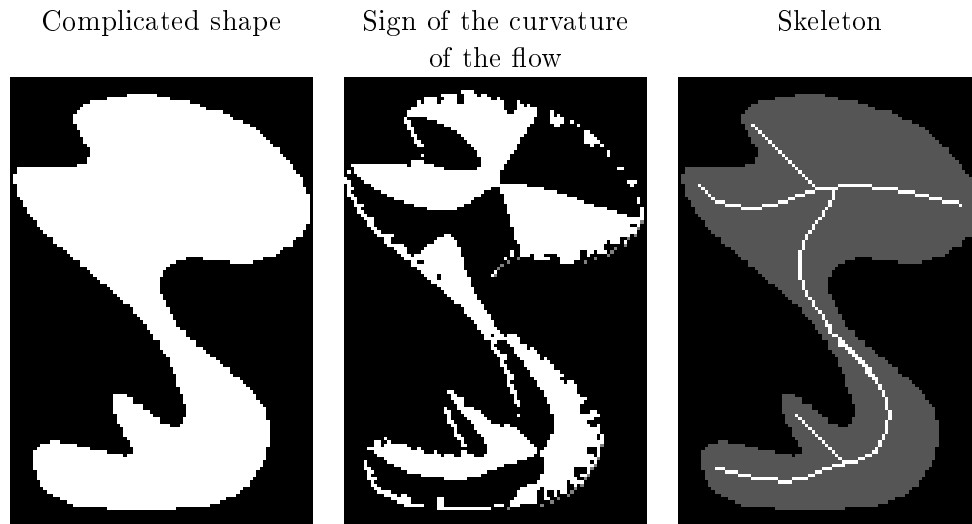


Figure 5: Skeleton computation of a complicated shape. Our algorithm works even in the case when the set of saddle points $F(5)$ is non empty.

- [4] H. Blum. Biological shape and visual science (part i). *J. Theor. Biol.*, 38:205–287, 1973.
- [5] H. Choi, S. Choi, and H. Moon. Mathematical theory of medical axis transform. *Pacific Journal of Mathematics*, 181(1):57–88, 1997.
- [6] P. Dimitrov. *Flux Invariants for Shape*. PhD thesis, McGill University, Department of Computer Science, Montréal, 2003.
- [7] P. J. Dimitrov, J.N. Damon, and K. Siddiqi. Flux invariants for shape. In *CVPR*, 2003.
- [8] L.C. Evans. *Partial Differential Equations*, volume 19 of *Graduate Studies in Mathematics*. American Mathematical Society, 1991.
- [9] D. Gilbarg and N.S. Trudinger. *Elliptic Partial Differential Equations of Second Order*, volume 28 of *Princeton Mathematical Series*. Springer-Verlag, 1970.
- [10] L. Gorelick, M. Galun, E. Sharon, R. Basri, and A. Brandt. Shape representation and classification using the poisson equation. *IEEE Transactions on Pattern Analysis and Machine Intelligence*, 28(12):1991–2005, 2006.
- [11] J. Hubbard and B. West. *Equations différentielles et système dynamique*. Enseignements des Mathématiques. Cassini, 1999.

- [12] I. Karatzas and S.E. Shreve. *Brownian Motion and Stochastic Differential Equation*. Springer Verlag, New York, 1988.
- [13] B. Kawohl. *Rearrangements and Convexity of Level Sets in PDE*, volume 1150 of *Lecture Notes in Mathematics*. Springer-Verlag, 2002.
- [14] R. Kimmel, D. Shaked, and N. Kiryati. Skeletonization via distance maps and level sets. *Computer Vision and Image Understanding*, 62(3):382–391, 1995.
- [15] M. Leyton. Symmetry-curvature duality. *Computer Vision, Graphics, and Image Processing*, 38:327–341, 1987.
- [16] L.G. Makar-Limanov. Solution of dirichlet’s problem for the equation $\Delta u = -1$ in a convex region. *Math. Notes of Acad. Sci. of U.S.S.R.*, 9:52–53, 1971.
- [17] G. Matheron. Examples of topological properties of skeletons. In Serra, editor, *Image Analysis and Mathematical Morphology*, volume 2, 1988. London Academic Press.
- [18] F. Meyer. Skeletons in digital spaces. In Serra, editor, *Image Analysis and Mathematical Morphology*, volume 2, 1988. London Academic Press.
- [19] L. Modica and S. Mortola. Il limite nella gamma-convergence di una famiglia di funzionali ellittici. *Boll. Un. Mat. Ita.*, 14A:526–529, 1977.
- [20] D. Pasquignon. Computation of skeleton by partial differential equation. In *ICIP*, 1995.
- [21] R.J. Di Perna and P.L. Lions. Ordinary differential equations, transport theory and sobolev spaces. *Invent. Math*, 98:511–547, 1989.
- [22] J. Serra. *Image Analysis Mathematical Morphology*, volume 2. Harcourt Brace Jovanovich, 1988.
- [23] J. Shah. Gray skeletons and segmentation of shapes. *Computer Vision and Image Understanding*, 99(1):96–109, 2005.
- [24] K. Siddiqi, S. Bouix, A. Tannenbaum, and S. Zucker. Hamilton-jacobi skeletons. *International Journal of Computer Vision*, 48(3):215–231, 2002.
- [25] S. Tari, J. Shah, and H. Pien. Extraction of shape skeletons from greyscale images. *Computer Vision and Image Understanding*, 66:133–146, 1997.
- [26] H. Tek and B.B. Kimia. Symmetry maps of free-form curve segments via wave propagation. In *ICCV*, pages 362–369, 1999.

- [27] X. You, Y.Y. Tang, W. Zhang, and L. Sun. Skeletonization of character based on wavelet transform. In *CAIP*, pages 140–148, 2003. LNCS 2756.